JOURNAL DE PHYSIQUE
Colloque C2, Supplément au n°6, Tome 49, juin 1988

NONLINEAR OPTICAL EFFECTS AT THE FUNDAMENTAL ABSORPTION-EDGE OF WIDE-GAP II-VI SEMICONDUCTORS

F. HENNEBERGER, J. PULS, H. ROSSMANN, M. KRETZSCHMAR, C. SPIEGELBERG and A. SCHÜLZGEN

Humboldt-Universität zu Berlin, Sektion Physik, Bereich 05, Halbleiteroptik, Invalidenstr. 110, DDR-1040 Berlin, D.R.G.

Abstract: This papers summarizes recent results on nonlinear absorption and refraction, optical switching bistability and digital logics at visible wavelengths using wide-gap semiconducting compounds.

1 - INTRODUCTION

Previous studies /1,2/ have shown that very strong and fast optical nonlinearities occur near the fundamental absorption edge of the wide-gap II-VI semiconductors at room temperature. They are related to the disappearance of the exciton resonances due to free carrier screening and make these materials good candidates for optical signal processing applications in the visible spectral range. This paper summarizes some results of more recent studies in this area.

2 - NONLINEAR ABSORPTION AT mW-POWER LEVELS

Previously /1,3,4/ we have demonstrated saturable absorption of CdS, CdSe and the corresponding mixed crystals in a near steady- state regime both in excite and-probe and single-beam experiments with nanosecond dye laser pulses at intensities of a few kW/cm^2. Those intensities are gainable by the output of cw laser sources focused on spots of some μm diameter and, in fact, we have recently succeeded in achieving full steady-state operation of the nonlinearity with the Argon-Ion laser. By means of an acousto-optical modulator 50 ns pulses were formed. The nonlinear transmission at two laser lines is shown in Fig. 1 . Bleaching of absorption at mW-power levels is clearly seen. This is one of the rare examples where a fast optical nonlinearity of electronic origin can be operated with cw lasers at room temperature. Since the switching times are clearly pico- and subpicosecond (see below) the switching energy is on the fJ-scale. Using the Ar^+ laser in a modelocked regime or the ps-YAG laser all-optical logic operations (AND, OR) have been performed in a pulsed mode. Current work concentrates on heat reduction to increase cycle rates.

3 - DEGENERATE FOUR WAVE MIXING AND NONLINEAR REFRACTION

Any change of absorption is accompanied by a corresponding change of refraction. A Kramers-Kronig analysis /2,5/ of nonlinear absorption data has yielded values as large as $6 \times 10^{-19}\ cm^3$ for the change of refraction δn induced by one electron-hole pair per cm^3 in CdS. However, the accuracy of Kramers-Kronig calculations is somewhat questionable, since there can be weak, but very long-ranged non-resonant absorption changes. In order to confirm this large nonlinear refraction experimentally, we have carried out degenerate four- wave mixing experiments. Two beams of equal intensity I_o from a dye laser operating at a power-level of some kW and pulse durations of ≈4ns were made to interfere on a 1.0 μm CdS platelet under a certain angle. The period of the resulting grating was about 20 μm, which is clearly larger than the carrier diffusion length. The intensities of the incoming beams as well as the transmitted (I_T) and the first-order four-wave mixing signals ($I_{p=1}$) were detected at the maximums of the pulses by fast Si-photodiodes and a boxcar integrator yielding a time resolution better than 1ns.

Fig. 2 presents the absolute four-wave mixing efficiencies observed scanning the frequency of the incoming light through the band-edge region. Maximum efficiency occurs somewhat below the groundstate exciton resonance

and a value of 5% is found at highest pump levels. For the ratio $I_{p=1}/I_T$ we get even values up to 20% around 2.5 eV. The scattering of the data at the low - energy side at highest pump is probably related to Fabry-Perot effects. Here, the refraction changes cause already substantial shifts of the interference fringes of the platelet-like sample. The pump intensity is that high that the nonlinearity is mainly due to bandfilling as evidenced by the

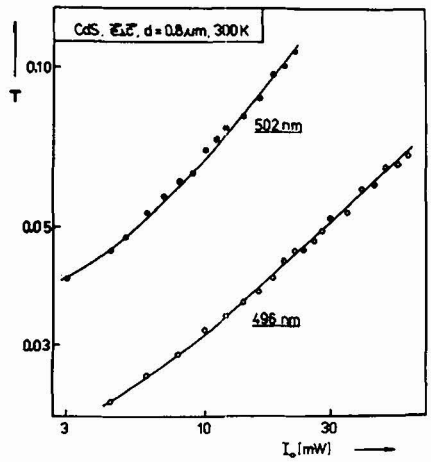

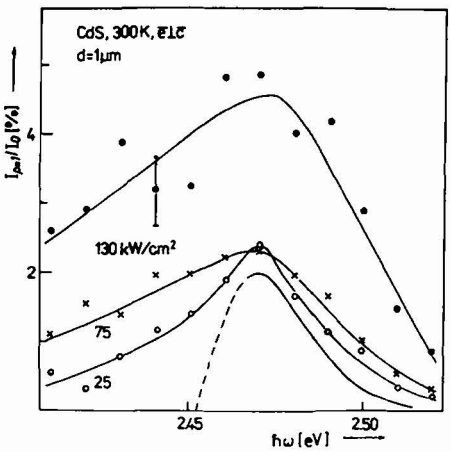

Fig. 1 Transmission of a 0.8 µm CdS sample at T=300 K versus input power at two wavelengths of the Ar^+ laser. Polarization perpendicular to the hexagonal axis.

Fig. 2 First-order degenerate four-wave mixing efficiency versus photon energy of a 1.0 µm thick CdS sample at T=300 K for three different input intensities. Polarization of all beams perpendicular to the hexagonal axis. Lowest curve: Calculated efficiency of the amplitude grating at 25 kW/cm² using the nonlinear absorption of /1,2/.

appearance of stimulation effects in the luminescence spectrum. In addition, pump depletion sets in. Therefore, for a detailed analysis we concentrate on lower pump levels. As known from earlier experiments /1,2/ there is strong nonlinear absorption decrease on the high-energy side . Using the respective data we have calculated the diffraction from the corresponding amplitude grating and good agreement with the experiment is obtained in this spectral range. On the other hand, only a weak absorption change is observed on the low energy side. Accordingly, the diffraction results here from a phase grating, from which one can determine the change of refraction Δn. Δn between the dark and bright spots of the interference grating is given by /6/

$$2\Delta n = 2(\lambda/d)\,[\,(1-R)^{-2}\exp(\alpha d)\,I_{p=1}/I_o\,]^{1/2} \qquad (1)$$

(R=0.2 is the reflection, d = 1 µm the sample thickness , and α the linear absorption measured simultaneously). In addition, the carrier density at the interference maximums can be estimated from

$$n_f = 4\,I_o\,(1-R)(\tau/\hbar\omega\, d)\,[\,1-\exp(-\alpha d)\,]. \qquad (2)$$

(τ is the carrier life - time of 200 ps /1,2/.) Combining both equations we can deduce the change of refraction $\delta n = 2\Delta n/n_f$ induced by one electron-hole pair in 1 cm^3 . The result is shown in Fig. 3 and , in fact, values as large as predicted by the Kramers - Kronig analysis are found. Surprisingly, the nonlinear refraction decreases at higher pump. We attribute this to a transition to a bandfilling nonlinearity, which is not that effective than the excitonic one.

Our four-wave mixing studies demonstrate that CdS exhibits a very large nonlinear refraction at room temperature. Although our sample is very thin, efficiencies of some percent have been observed. The nonlinear refraction coefficient δn is as large as that of GaAs/GaAlAs multiple quantum wells /7/ . However, the present data have been obtained in a quasi steady-state regime; in a spectral range of substantially lower linear absorption

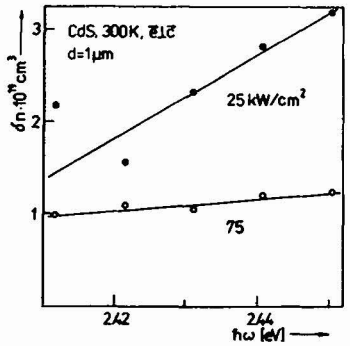

Fig. 3 Change of refraction per electron - hole pair per cm^3 at the low - energy side of the exciton groundstate resonance (E_x=2.475 eV) calculated from the data in Fig. 2 and (1) and (2).

and for a 100 times shorter recovery time. These large refraction changes make CdS a very good candidate for applications *in dispersive* optical bistability, phase conjugation, and other refractive switching techniques at visible wavelengths.

4 - FEMTOSECOND DYNAMICS

Picosecond excite and-probe measurements /2,8,9/ have yielded carrier-recombination controlled recovery of the nonlinearity within 200 ps. Switch-on occurred instantaneously with the pump pulse of 6 ps .Thus, the underlying process is shorter than this time and a a study on the *fs time-scale* is desirable.
Using the amplified output of a CPM laser ([1]) at 618 nm with a pulse duration of 115 fs we have studied in a excite- and-probe configuration:

(i) Below-gap , exciton resonant excitation of CdS_xSe_{1-x} matching x properly and
(ii) above-gap excitation of pure CdSe.

The pump polarization was chosen parallel to the crystal axis c, so that primary only B-holes were excited. In accord with earlier experiments on the *ns- and ps-time* scale /1,2/ we have observed in both situations a pronounced increase of the probe transmission , however, with a different time behaviour. For exciton-resonant

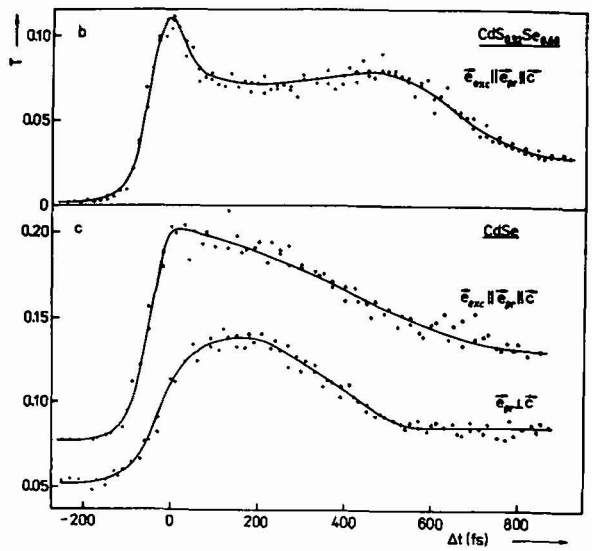

Fig. 4 Probe beam transmission versus pump-probe delay (Pump 1 mJ/cm^2 Probe: 0.01 mJ/cm^2).
a) B-exciton resonant excitation of CdS_xSe_{1-x} (thickness 3 μm). A value of x=0.34 is used to match the 618 nm laser output.
b) 250 meV above- gap excitation of CdSe (0.3 μm). All data at room temperature .

[1] The fs-studies have been performed in close cooperation with M. Rudolph and co-workers at the Friedrich-Schiller-Universität, Jena (GDR).

excitation (Fig. 4a) we find a distinct coherence peak, followed by a plateau and subsequent recovery with a time constant of about 250 fs. (On a commercial filter of CdS_xSe_{1-x} microcrystallites embedded in glass studied for comparison no recovery is seen within 1 ps). To separate coherent interaction and that originating from real carriers we have studied the first-order defraction from the transient grating produced by pump and probe together . A slight asymmetry of the efficiency (with respect to probe ahead or behind pump) is found, which we attribute to the exciton dephasing with a characteristic time of about 50 fs. Substracting the coherence part in Fig. 4a we get a switch-on time for the nonlinearity via carriers somewhat below 100 fs . Physicalty, this is the time necessary for the ionization of excitons by LO-phonon absorption resulting in free carriers screening out the exciton resonance. Simultaneously the gap shrinks, so that the actual band edge is below the excitation frequency at larger delays and a complex carrier dynamics sets in leading to a nearly constant probe transmission. The very fast recovery results from the decay of the non-thermal carriers at the excitation frequency down to the band bottoms (c.f. Fig. 4b). Note, that at room temperature there is no essential difference between the linear levels of the below-gap exciton and above-gap continuum absorption.

For 250 meV above-gap excitation of CdSe (Fig. 4b) no clear coherence peak is seen , since we produce directly carriers with very rapid dephasing: the first-order efficiency follows instantaneously the pump pulse in this case. We observe essentially the state-filling dynamics of the carriers studied at low temperature in /10/. However, we find different results for probe polarization parallel and perpendicular to c. In the first case (upper curve in Fig. 4b) the absorption blocking due to B-holes is probed and, accordingly, no delay of the respective transmision increase is seen. But, using probe polarization perpendicular c, we monitor the blocking due to A- holes, which, in fact, shows up delayed to that of B-holes. Thus, we have directly observed the B- to A-hole conversion in CdSe which takes about 80 fs.

The data in Fig. 4 directly demonstrate that the wide-gap II- VI's can be used for optical switching and logic operations in the subpicosecond range. High contrast, fs-recovery, and room temperature distinguish them from other materials.

5- OPTICAL BISTABILITY

The nonlinear absorption and refraction discussed above allows to achieve Fabry-Perot bistability on reflection coated samples. Operating at the exciton resonace ($\hbar\omega = 2.475$ eV at $e \perp c$) , where the absorption bleaching is maximum, we have demonstrated absorptive FP bistability in the kW/cm^2 intensity range on CdS at room temperature /1,2/.

The data in Chapter 2 suggest dispersive FP bistability far away from the exciton resonance. We have studied an etalon made from a dielectrically coated CdS sample the transmission peak of which is 70 meV(!) below the exciton resonance (see insert Fig. 5a). Since the nonlinear refraction is negative in this region, the laser was tuned on the high energy side, so that the peak runs to the laser frequency with rising intensity. The shapes

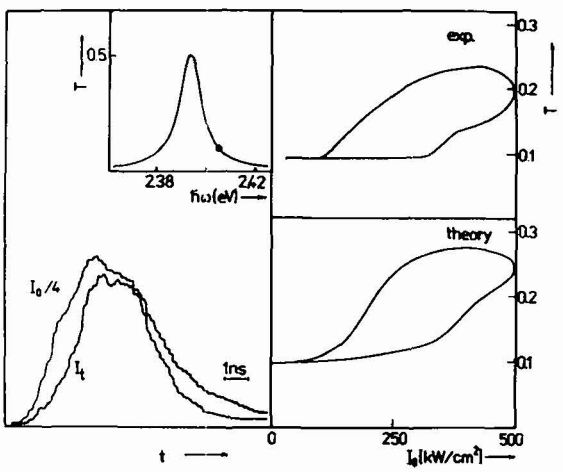

Fig. 5 Dispersive Fabry—Perot bistability on dielectrically coated CdS (d=1.1μm) at room temperature. Explanations see text.

of the incident and transmitted pulse is shown in the lower left and the corresponding transmission versus input intensity loop in the upper right part of Fig. 5, respectively. Hysteresis occurs only above some certain peak intensity, while nonlinearity is already observed at smaller inputs. Thus, the loop in Fig. 5 is not a simple transient one. However, no clear switching is seen. This is due to transverse effects, because the spot (≈ 35 μm) is much larger than the carrier diffusion length. This is confirmed by a respective calculation /11/ treating the full spatial (in both directions parallel and perpendicular to the beam) and time problem for the carrier density and light intensity. The result is presented in the lower right part of Fig. 5 and good agreement with the experimental loop is seen. The only free parameter is the carrier diffusion length for which a value of 1μm is used being in reasonable accord with literature data /12/. The intensities needed to get bistability are more than 10 times larger as compared to the absorptive case /1,2/. However, since only 8% of the input intensity are absorbed, the energy consumption is equal for both kinds of bistabilities. Similar bistable behaviour at thicker samples and higher intentensities has been reported in /13/.

The nonlinear Fabry-Perot cavity is only one way to achieve bistability and for both fundamental and practical reasons, there is an extensive search for new concepts , which do not require external mirrors. One of the most easy ways to achieve mirrorless bistability is increasing absorption (see e.g. /14/). However, from a practical point of view the high absorption necessarily involved is of disadvantage . Several papers (for references see /14/ or /15/) have proposed and partly demonstrated dispersive cavityless bistability, but none of them is substantially superior to the Fabry-Perot cavity. A virtually simple concept would be nonlinear reflection at the boundary between different media provided positive feedback can be put into action. That concept has been

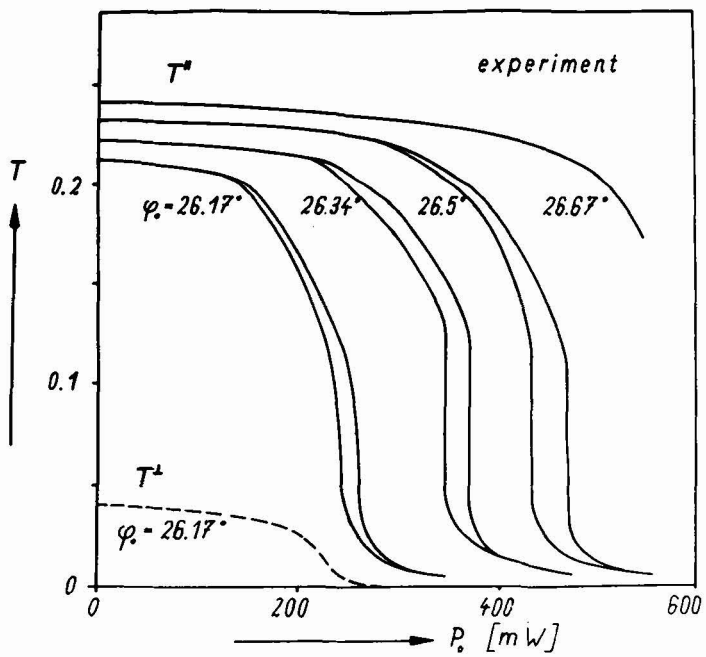

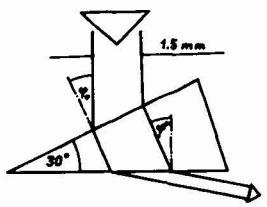

Fig. 6a Schematics of the nonlinear (ZnSe) prism used for mirrorless dispersive bistability.

Fig. 6b Transmission through the above prism versus input power for input polarization parallel ($T_{\parallel}$) and perpendicular ($T_{\perp}$) to the plane of incidence, respectively. $\lambda = 514$ nm

firstly used in /16 / , where the specific situation of total-reflection incidence on an optically thin medium with nonlinear refraction has been considered. We have recently proposed and demonstrated /15/ a new kind of mirrorless dispersive bistability also based upon nonlinear reflection, but distinctly different to that of /16/. The general schematics of that bistability is shown Fig.6a. At first sight it looks similar to that used in /16/, but in these studies the nonlinear medium is placed *under* the output face of the prism. The latter is only needed to achieve total reflection at the nonlinear interface at low intensities. In contrast, we consider the situation, where the prism itself presents the nonlinear medium merely surrounded by air. A second point crucially for the bistability presented here is that we use an input beam polarized in the plane of incidence. Then, the reflection at the prism output face changes drastically (ideally between Zero and unity) when the angle of incidence is tuned from the

Brewster angle φ_B into that for total reflection φ_T. For the prism we use a medium with positive nonlinear refractior $n=n_1+n_2 I$. Accordingly, φ_B and φ_T move to lower angles with rising light intensity I. The input beam is now impinged on the prism in a way yielding $\varphi_B \approx \varphi^* < \varphi_T$ at low intensities, φ^* is the angle of incidence on the prism output face. That is, the light incident on the output face of the prism is almost fully transmitted and the nonlinearity is only driven by the input beam ($I \approx I_o$). Increasing of the input intensity increases the actual n, whereby φ_B shifts offwards but φ_T towards φ^* and the reflection increases. The reflected light increases in turn the refraction index of the prism, so that φ_T approaches more closely φ^* resulting in a further increase of the reflection and so on. If the reflection increase is steep enough this feedback becomes regenerative leading to runaway and switching to total reflection. Now the nonlinearity is pumped by the incoming and reflected beam ($I \approx I_o + I_R \approx 2I_o$). When the input intensity is subsequently reduced the reflected signal helps the prism to maintain total reflection resulting in optical hysteresis. For the experimental demonstration of this bistability we have used a ZnSe prism and the 514 nm line of the Ar^+ laser ($\varphi_B = 19.78°$). The nonlinearity is of thermal origin. A detailed theoretical analysis /15/ shows that bistability is expected for input angles φ_o larger than 26° for the prism apex angle of 30° used. Indeed, we find in the experiment clear hysteresis just in that range of input angles (Fig. 6b). To check, wether this is not simply increasing absorption bistability we have tuned the polarization of the input beam in the direction perpendicular to the plane of incidence and, as expected, hysteresis disappeared. Bistable switching at angles of incidence larger than 27° could not be demonstrated because of the available maximum power of the laser. Note, however, that the intensity on the sample is as low as 8 W/cm^2 since we operate without focusing. Hysteresis occurs also in the output angle. This feature is different to the Fabry-Perot cavity and of practical importance, since it can be used in several ways to direct or adress beams . In addition, the advantage of this bistability in comparison to the previously studied bistability at total reflection /16/ is that we operate in a regime, where the input light penetrates fully into the nonliniear medium and , thus, pumps much more effectively.

The cavityless dispersive bistability demonstrated above shows another useful property of the wide-gap II-VI semiconductors. These materials make available thermo-optic nonlinearities at the wavelengts of the Ar ion laser. Therefore, they are well suited to study in an easy way the behaviour of bistable systems or to demonstrate even new types of optical bistabilities.

REFERENCES

/1/ Henneberger, F., Puls, J., and Spiegelberg, Ch., Optical Bistability III, Ed. Gibbs, H.M., Mandel, P., Pheyghambarian, N.,and Smith, S.D., Springer-Verlag 1985 (p. 156).

/2/ Henneberger, F., Puls, J., Rossmann, H., Spiegelberg, Ch., Kretzschmar, M., and Haddad, I., Proc 6.th General Conf. Condensed Matter Division Europian Phys.Soc., Physica Scripta T13 (1986) 195.

/3/ Puls, J. and Henneberger, F., phys. stat. sol. (b) 121 (1984) K187.

/4/ Henneberger, F., Puls, J., and Rossmann, H., J. Lum. 30 (1985) 204.

/5/ Henneberger, F., Woggon, U., Puls, J., and Spiegelberg, Ch., Appl. Phys. B 45 (1988) in press.

/6/ Eichler, H.J., Festkörperprobleme 18 (1978)241.

/7/ Miller, D.A.B., Chemla, D., Eilenberger, D.J., Smith, P.W., Gossard, A.C. and Wiegmann, W., Appl.Phys. Letters 42 (1983) 295.

/8/ Puls, J., Fink, F., and Henneberger, F., Proc. Internat. Symp. Ultrafast Phenomena Spectroscopy, Minsk 1983, p. 339.

/9/ Puls, J., Henneberger, F., Fink, F., and Jüpner, I., Proc. Internat. Symp. Ultrafast Phenomena Spectroscopy, Reinhardsbrunn (GDR),1985 p. 339.

/10/ Peyghambarian,N., and Koch, S.W., Rev. Phys. Appl. 22 (1987).

/11/ Kretzschmar, M., thesis, Humboldt-Universität, Berlin 1988.

/12/ Saito,H.,and Göbel,E.O., Phys.Rev.B 318(1985)2360.
Majumder,F.A., Swoboda,H.E., Kempf,K., and Klingshirn,C., Phys.Rev. B32(1985)2407.

/13/ Wegener, M., Klingshirn,C., Koch, S.W., and Banyai,L., Semicond. Sci.Technol.1 (1986)366.

/14/ Henneberger,F., phys. stat. sol. (b) 137 (1986) 371.

/15/ Henneberger, F., Rossmann,H., and Schülzgen,A., phys. stat. sol. (b) 145(1988)K83.

/16/ Smith, P.W., Tomlinson, W.J., Maloney, P.J.,and Hermann, J.P., IEEE J. Quantum Electronics 17 (1981) 381.